Hindawi
Journal of Nanomaterials
Volume 2019, Article ID 8524950, 8 pages
https://doi.org/10.1155/2019/8524950

Research Article

Synthesis and Characterization of High-Purity Ultrafine Platinum Particles by Chemical Refining Method

Panchao Zhao,[1,2] **Wei Yi**,[1,2] **Qigao Cao**,[1] **Bosheng Zhang**,[1] **Kunkun Chen**,[1] **Jigang Li**,[2] **and Chensiqi Yao**[2]

[1]*Northwest Institute for Non-ferrous Metal Research, Xian 710016, China*
[2]*Kunming Institute of Precious Metals, Kunming 650106, China*

Correspondence should be addressed to Panchao Zhao; 564070695@qq.com

Received 15 October 2018; Accepted 23 December 2018; Published 25 March 2019

Academic Editor: Vincenzo Baglio

High-purity ultrafine platinum particles are widely used to fabricate platinum electrode oxygen sensors for automobiles and thick-film platinum resistance temperature elements. In this study, the near-spherical ultrafine Pt particles of high purity were synthesized by chemical purification, spray-drying, and ignition from crude Pt powder. Impurities in the initial Pt powder were eliminated by the 001×7 strong acid cation resin exchange column and precipitation treatment. Near-spherical $(NH_4)_2PtCl_6$ particles were obtained after spray-drying, and then the microstructure and size of as-synthesized Pt particles were controlled by the ignition process. The influences of different heating temperatures during ignition treatment on the microstructure and size of Pt particles were investigated. The purity of as-synthesized Pt particles was higher than 99.999 wt%, and the average size was about 1.12 μm. The results indicate that high-purity ultrafine Pt particles can be efficiently synthesized by chemical refining.

1. Introduction

Ultrafine platinum powder is a kind of material with high chemical activity. The application of ultrafine Pt powder as a microelectronic material (platinum electronic paste) and catalytic material is expanding rapidly [1–7]. Pt electronic paste is mainly used to prepare platinum electrode oxygen sensors for automobiles and thick-film platinum resistance temperature elements [8–10]. It is known that the Pt electronic paste is composed of ultrafine Pt particles, organic carriers, and binders [9]. Therefore, the properties of ultrafine Pt particles have a great influence on the properties of Pt materials fabricated by Pt electronic paste. In general, the preparation of Pt electronic paste has higher requirements for Pt particles [9, 11], such as the narrow average distribution ranging from 0.1 to 3 μm, homogeneous and near-spherical grain morphology, good dispersion and no agglomeration, low impurity content, and high density, which are strictly required. So, a suitable Pt powder plays a key role in preparing Pt electronic paste. At present, a suitable Pt powder for Pt electronic paste is mainly synthesized by the liquid chemical reduction method [6, 7, 12]. However, the liquid chemical reduction method has several limitations in terms of agglomeration, the purity of Pt powder, and the production of a large amount of waste liquor. Hence, it is very important to develop an appropriate combined approach (chemical method combined with other methods) to solve the above drawbacks.

Spray-drying is a known method for producing spherical particles due to the instantaneous transition from the liquid (solvent) to the solid (solute) phase [13–19]. Compared with other drying technologies, spray-drying is clean, rapid, reproducible, inexpensive, and easily scaled up, which is why it is widely used in industrial milling [14, 17, 18]. During the process of spray-drying, the solution (solute-solvent) is completely atomized and dispersed into the chamber (hot gas) when interacted with the high-pressure gas at the nozzle. Afterward, the atomized fogdrops evaporate in the drying

chamber and form spherical or near-spherical solid particles simultaneously. The powder prepared by spray-drying has high dispersibility and good sphericity and homogeneity [13, 18, 19]. Moreover, it is of high purity since no impurity is introduced during the spray-drying stage. The particle size distribution ranging from 0.5 to 5 μm can be obtained by controlling spray-drying parameters, because the result is heavily affected by the parameters [19]. Therefore, spray-drying is an effective way to prepare a high-purity ultrafine powder [18, 19].

In this study, the high-purity ultrafine Pt particles were prepared by the spray-drying method combined with chemical purification from crude platinum powder (≤99.9%). The purity of the Pt powder separated by chemical purification was higher than 99.999 wt%, and an ultrafine Pt powder was obtained after the spray-dried ammonium hexachloroplatinate ($(NH_4)_2PtCl_6$) particles as intermediates were ignited in a pipe furnace in N_2/H_2 (vol. 5 : 5). To the best of our knowledge, there are no reports about preparing high-purity ultrafine Pt particles by spray-drying. So, in the present work, the parameters of the calcination process are intensively studied to understand the synthesis mechanism of high-purity ultrafine Pt particles in depth.

2. Materials and Methods

All reagents and solvents were used as received without further purification. Crude platinum powder (≤99.9%) was purchased from Sino-Platinum Metals Co. Ltd. (Yimen, Yunnan, P.R. China); 001 × 7 strong acid cation resin was purchased from Langfang City Nanda Resin Co. Ltd. (Langfang, Hebei, P.R. China); and guaranteed high-grade sodium hydroxide (NaOH), sodium chloride (NaCl), ammonium chloride (NH_4Cl), hydrochloric acid (37.5 wt%, HCl), and nitric acid (66.5 wt%, HNO_3) were purchased from Sigma-Aldrich (St. Louis, MO). Deionized water was used as the solvent.

The crude Pt powder was dissolved in aqua regia solution (HCl/HNO_3, vol. 3 : 1) and heated from room temperature to 90°C, from which the H_2PtCl_6 solution can be obtained. Then, hydrochloric acid (6 mol/L) was constantly added into the H_2PtCl_6 solution, and the mixed solution was heated to boiling repeatedly to remove nitrate, by which the pH value of the solution was adjusted to 1.5. The base metal cation impurities were removed after the nitrate-removed H_2PtCl_6 solution (pH value ≈ 1.5) slowly passed through the 001 × 7 strong acid cation resin exchange column. The process of removing impurities was repeated after the pH value of the H_2PtCl_6 solution was adjusted to 3, by which the noble metal impurities could be removed. High-purity $(NH_4)_2PtCl_6$ powder was precipitated by adding a saturated NH_4Cl solution to the H_2PtCl_6 solution. Then, the $(NH_4)_2PtCl_6$ precipitation dissolved in distilled water was spray-dried to microspherical particles. Subsequently, high-purity microspherical $(NH_4)_2PtCl_6$ particles were ignited in N_2/H_2 (vol. 5 : 5) at 500°C for 30 min followed by cooling under N_2/H_2, and the high-purity ultrafine Pt particles were synthesized.

Table 1: Element analysis of the as-synthesized platinum powder.

Elements	Raw platinum	As-precipitated $(NH_4)_2PtCl_6$	As-synthesized platinum
Main (wt%)			
Pt	<99.9	43.95	>99.999
Impurity (ppm)			
Na	180.1	1.1	1.9
K	45.3	<1	<1
Ca	238.2	1.7	2.6
Al	110.3	<1	<1
Mg	155.5	<1	<1
Fe	281.3	1.2	1.8
Si	143.2	1.3	1.9
Cr	23.6	<1	<1
Cu	122.5	<1	<1

The purity of as-synthesized $(NH_4)_2PtCl_6$ powder was measured by inductively coupled plasma-atomic emission spectrometry (ICP-AES, Optima 5300 DV, PerkinElmer, USA). A commercial spray-drying machine (B290, BUCHI, Switzerland) was used to synthesize high-purity microspherical $(NH_4)_2PtCl_6$ particles. The purity of crude Pt powder and high-purity ultrafine Pt particles were analyzed by inductively coupled glow discharge mass spectrometry (GD-MS, GD Plus GD, Element™, Thermo Fisher Scientific, USA), respectively. The solid phases in different stages were characterized by X-ray diffraction (XRD, Empyrean, PANalytical, the Netherlands, CuKα radiation at 40 kV). The microstructures of $(NH_4)_2PtCl_6$ particles and thermally decomposed products were observed by field emission scanning electron microcopy (FE-SEM, S-4800, Hitachi, Japan). The average particle size and size distribution of the as-synthesized Pt powder were obtained by a laser particle size analyzer (Mastersizer 3000, Malvern, UK).

3. Results and Discussion

3.1. Elemental Analysis. The elemental analysis results of crude Pt powder, chemically precipitated powder of $(NH_4)_2PtCl_6$, and as-synthesized Pt particles are shown in Table 1, where Pt and several impurity elements are listed. The purity of crude Pt powder was lower than 99.9 wt%, because the impurities in the initial Pt powder exceeded 500 ppm. In the chemical precipitation powder of $(NH_4)_2PtCl_6$ obtained by the chemical purification method, all the element contents of the impurities were effectively decreased to lower than 10 ppm (the Na, Ca, Fe, and Si contents were 1.1, 1.7, 1.2, and 2.9 ppm, respectively). The Pt content in the compound was 43.95 wt%, which coincided with the theoretical stoichiometric ratio of the $(NH_4)_2PtCl_6$ compound. As a result, the purity of as-synthesized Pt particles was higher than 99.999%, and the impurity contents of Na, Ca, Fe, and Si were 1.9, 2.6, 1.8, and 1.9, respectively. The impurity contents of as-synthesized Pt particles combined with the chemical

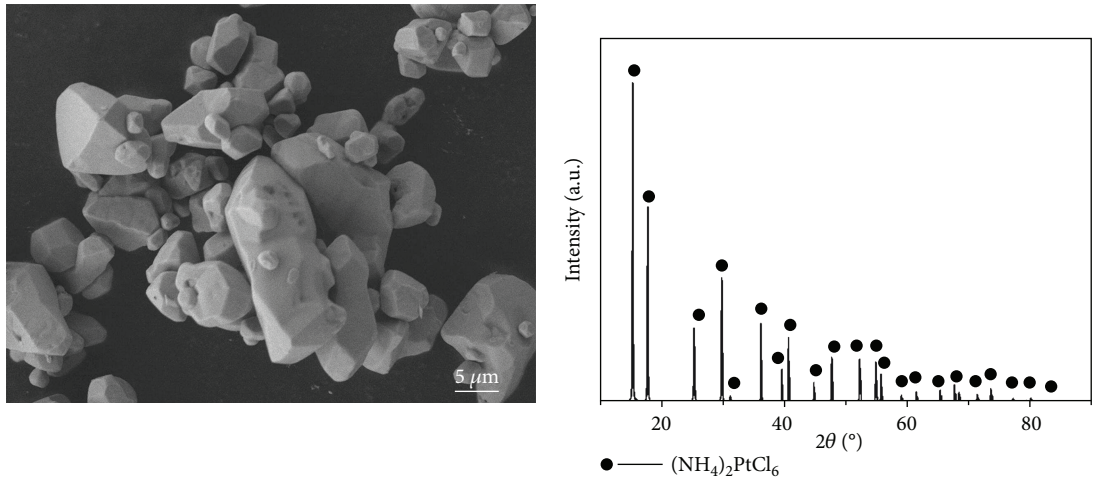

Figure 1: The microstructure and XRD pattern of as-precipitated $(NH_4)_2PtCl_6$ powders.

precipitation powder of $(NH_4)_2PtCl_6$ were slightly increased, because the amount of impurities did not change and the total mass was reduced when $(NH_4)_2PtCl_6$ particles were sintered. Therefore, the impurities in the raw Pt powder could be effectively reduced through the chemical purification process.

3.2. As-Precipitated $(NH_4)_2PtCl_6$ Analysis. The microstructure of the precipitates is shown in Figure 1(a), where a lot of blocks consisting of three-dimensional irregular polyhedrons of micron size are observed. In order to control the high-purity property of precipitation, no other reagent was added. Thus, the as-precipitated $(NH_4)_2PtCl_6$ shows its natural microstructure. The XRD pattern of the chemical sediment (after the precipitation process) is shown in Figure 1(b). All diffraction peaks of the chemical sediment can be found in the International Centre for Diffraction Data (formerly Joint Committee on Powder Diffraction Standards JCPDS 7-240 database) [20], and the chemical sediment is identified as $(NH_4)_2PtCl_6$.

3.3. Spray-Drying Process Analysis. The precipitated $(NH_4)_2PtCl_6$ powder was dissolved in deionized water with a certain concentration and heated to 85°C to dissolve sufficiently. The schematic representation of the typical process wherein the solution of the precursors is atomized into fogdrops by a two-fluid nozzle is shown in Figure 2(a). The solution and high-pressure gas (air or nitrogen) interact at the nozzle due to their high relative speed, and then the solution is crashed into a lot of small fogdrops in the drying chamber. Subsequently, the atomized fogdrops are instantaneously dried into microsized near-spherical solid particles in the spray-drying chamber where the temperature is 180°C. As shown in Figure 2(b), the microsized near-spherical $(NH_4)_2PtCl_6$ powder was prepared by spray-drying. The microstructure of the spray-dried $(NH_4)_2PtCl_6$ powder contains a lot of pores and regular blocks, because during the spray-drying process, the crystallized $(NH_4)_2PtCl_6$ on the surface is broken by the water vapour in the fogdrops, and then the broken crystal $(NH_4)_2PtCl_6$ grows again. All diffraction peaks of the spray-dried powder (in Figure 2(c)) can be found in the International Centre for Diffraction Data and can be identified as $(NH_4)_2PtCl_6$, which shows that all the spray-dried $(NH_4)_2PtCl_6$ particles are crystallized perfectly. The particle size distribution of the spray-dried $(NH_4)_2PtCl_6$ powder was between 0.5 and 3.5 μm, and the mean size was about 1.85 μm (in Figure 2(d)).

3.4. The XRD Pattern Analysis. The thermal behavior of $(NH_4)_2PtCl_6$ was studied in depth by Yılmaz and Içbudak [21]. Yılmaz and Içbudak had pointed out that $(NH_4)_2PtCl_6$ decomposes in two stages: the first stage takes place when the temperature ranges from 279°C to 345°C and the second stage takes place when the temperature ranges from 345°C to 410°C. In this study, the spray-dried $(NH_4)_2PtCl_6$ powder was ignited in N_2/H_2 (vol. 5 : 5) at different temperatures (300°C, 345°C, 380°C, and 410°C, respectively) for 30 min with a heating rate of 5°C/min, and the solid phases in different stages were characterized by X-ray diffraction. Figures 3(a)–3(d) show the X-ray diffraction patterns of the products at four different temperatures of 300°C, 345°C, 380°C, and 410°C, respectively. The product ignited at 300°C for 30 min consisted of both $(NH_4)_2PtCl_6$ and $Pt(NH_3)_2Cl_4$ phases, which can be seen in Figure 3(a). The newly generated $Pt(NH_3)_2Cl_4$ phase is very weak, and the $(NH_4)_2PtCl_6$ can decompose at 300°C but only a little. When the temperature reached 345°C, the phases of $(NH_4)_2PtCl_6$, $Pt(NH_3)_2Cl_4$, Pt, and $PtCl_2$ could be found as shown in Figure 3(b), respectively. In addition, the phase of $PtCl_2$ was very weak compared with the other phases, and the phase of $Pt(NH_3)_2Cl_4$ became stronger. It is indicated that the thermal decomposition of $(NH_4)_2PtCl_6$ is very intense at 345°C, and $Pt(NH_3)_2Cl_4$ as an intermediate product might decompose into Pt and $PtCl_2$ phases. When the temperature

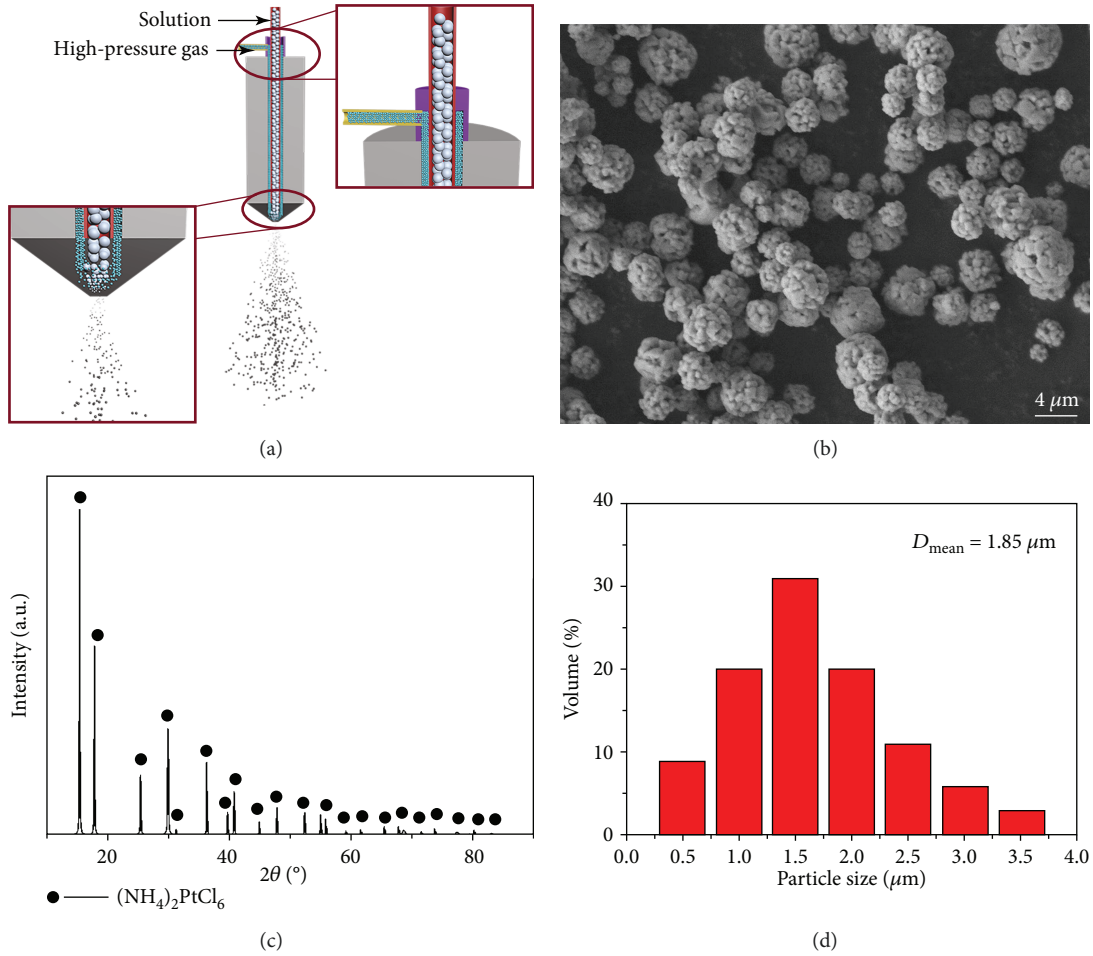

Figure 2: Spray-drying synthesis of microsized $(NH_4)_2PtCl_6$ powder with near-spherical particles: (a) schematic showing the spray-drying process used to synthesize the near-spherical powder, (b) the microstructure of spray-dried $(NH_4)_2PtCl_6$ powder, (c) the XRD pattern of spray-dried $(NH_4)_2PtCl_6$ powder, and (d) the particle size distribution of spray-dried $(NH_4)_2PtCl_6$ powder.

increased to 385°C, the phases of Pt and $PtCl_2$ were still observed, but the phases of $(NH_4)_2PtCl_6$ and $Pt(NH_3)_2Cl_4$ disappeared (in Figure 3(c)). At this stage, $(NH_4)_2PtCl_6$ and $Pt(NH_3)_2Cl_4$ were completely transformed into Pt and $PtCl_2$, and the remaining Pt compounds were mostly Pt and a little $PtCl_2$ phase. All the diffraction peaks of the samples treated at 410°C for 30 min presented in Figure 3(d) were the typical Pt XRD peaks, and no other peaks existed. It is concluded that the Pt compounds can be completely transformed into a Pt metal at 410°C.

3.5. Microstructural Characterization. According to XRD analysis, the microstructures of the thermally decomposed products of $(NH_4)_2PtCl_6$ powder at different calcination temperatures (300°C, 345°C, 380°C, 410°C, 450°C, and 500°C, respectively) are shown in Figure 4. The typical FE-SEM images of the microstructures of Pt compounds with high magnification are observed. In this part, the reduction process had the same parameters as the thermal decomposition process, and two experiments at two different igniting temperatures (450°C and 500°C, respectively) were added. After treatment at 300°C for 30 min, the $(NH_4)_2PtCl_6$ powder just began to decompose and its microstructure was almost the same as that of spray-dried $(NH_4)_2PtCl_6$ particles (in Figure 4(a)). However, the surface of products with many nanopores changed slightly because of the release of thermally decomposed gases (NH_3 and HCl), as shown in Figure 4(a) (top left corner). When the temperature reached 345°C, the thermal decomposition of Pt compounds was very intense, and more gas was rapidly released. The volume of Pt compounds compared with products ignited at 300°C shrank and became more densified, and there were many nanopores and numerous nanoparticles in the surface of Pt compounds as can be seen in Figure 4(b). According to XRD analysis, the Pt compound contained the $(NH_4)_2PtCl_6$, $Pt(NH_3)_2Cl_4$, Pt, and $PtCl_2$ phases at 345°C. The newly generated Pt compounds gathered to form a compact structure, and especially newborn Pt atoms agglomerated into nanoparticles due to the high energy of newborn Pt atoms. As the heating temperature increased to 380°C, the products were composed of Pt and a little $PtCl_2$ according to XRD analysis. At this stage, as $(NH_4)_2PtCl_6$ and $Pt(NH_3)_2Cl_4$ were transformed into Pt

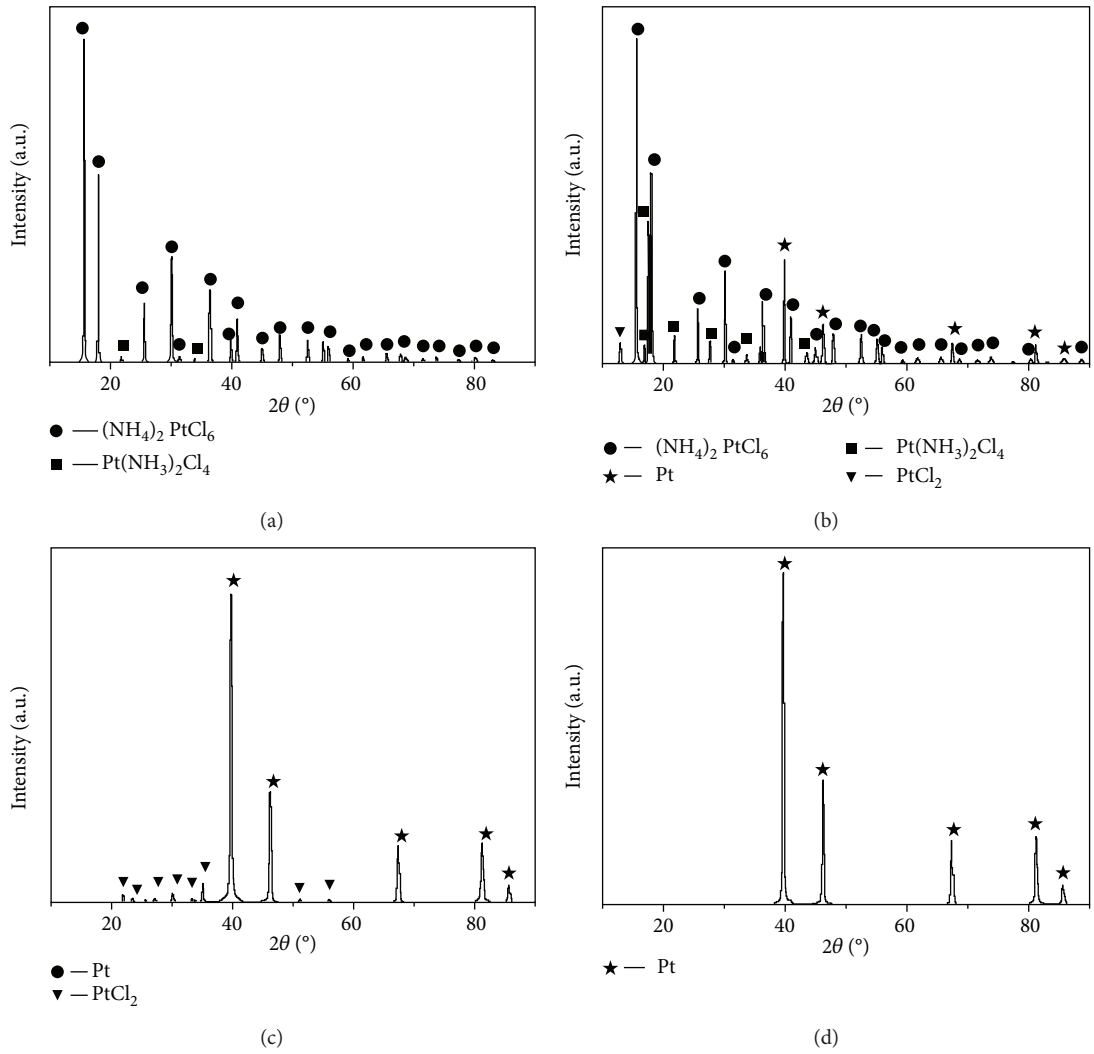

FIGURE 3: The XRD patterns of different thermal decomposition products of spray-dried $(NH_4)_2PtCl_6$ powder heated at (a) 300°C, (b) 345°C (new Pt compounds), (c) 385°C (newborn Pt), and (d) 410°C (Pt).

and $PtCl_2$ and the newborn Pt atoms grew into nanoparticles simultaneously, a microsized Pt metal framework composed of Pt nanoparticles (approximately 15 nm) with a large number of mesoporous material was formed, as shown in Figure 4(c). When the temperature was continually being heated to 410°C, the remains were totally transformed into pure Pt according to XRD analysis. Figure 4(d) shows the microstructure of the Pt particles at 410°C. The microsized Pt metal framework with mesoporous materials became more clearly observable, and the Pt nanoparticle size became enlarged to approximately 40 nm because the number of newly generated Pt atoms increased and the growth of Pt nanoparticles continued. Simultaneously, a few amounts of Pt lumps (approximately 1 μm) were formed by the gathering and growth of newly generated Pt nanoparticles which were unstable and had high activity at a higher sintering temperature. When the igniting temperature increased to 450°C, there was no chemical reaction at this stage but there were physical changes. Obviously, the number of Pt metal frameworks with mesoporous materials decreased, while the quantity of microsized Pt particles increased, as shown in Figure 4(e). This was due to the unstable Pt nanoparticles which had higher activity at a higher temperature (450°C) and were easier to sacrifice to form microsized Pt particles. Finally, the unstable Pt nanoparticles were completely transformed into microsized Pt particles which were near spherical, well dispersed, and densified (in Figure 4(f)). The particle size distribution of Pt powder is shown in Figure 5, and the average size is about 1.12 μm with a particle size distribution between 0.2 and 1.8 μm. It is indicated that the near-spherical ultrafine Pt particles with good dispersity were obtained.

4. Conclusions

In summary, the high-purity (99.999 wt%) $(NH_4)_2PtCl_6$ particles can be obtained from crude Pt powder (99.9 wt%) by the chemical purification method. Then, the microsized

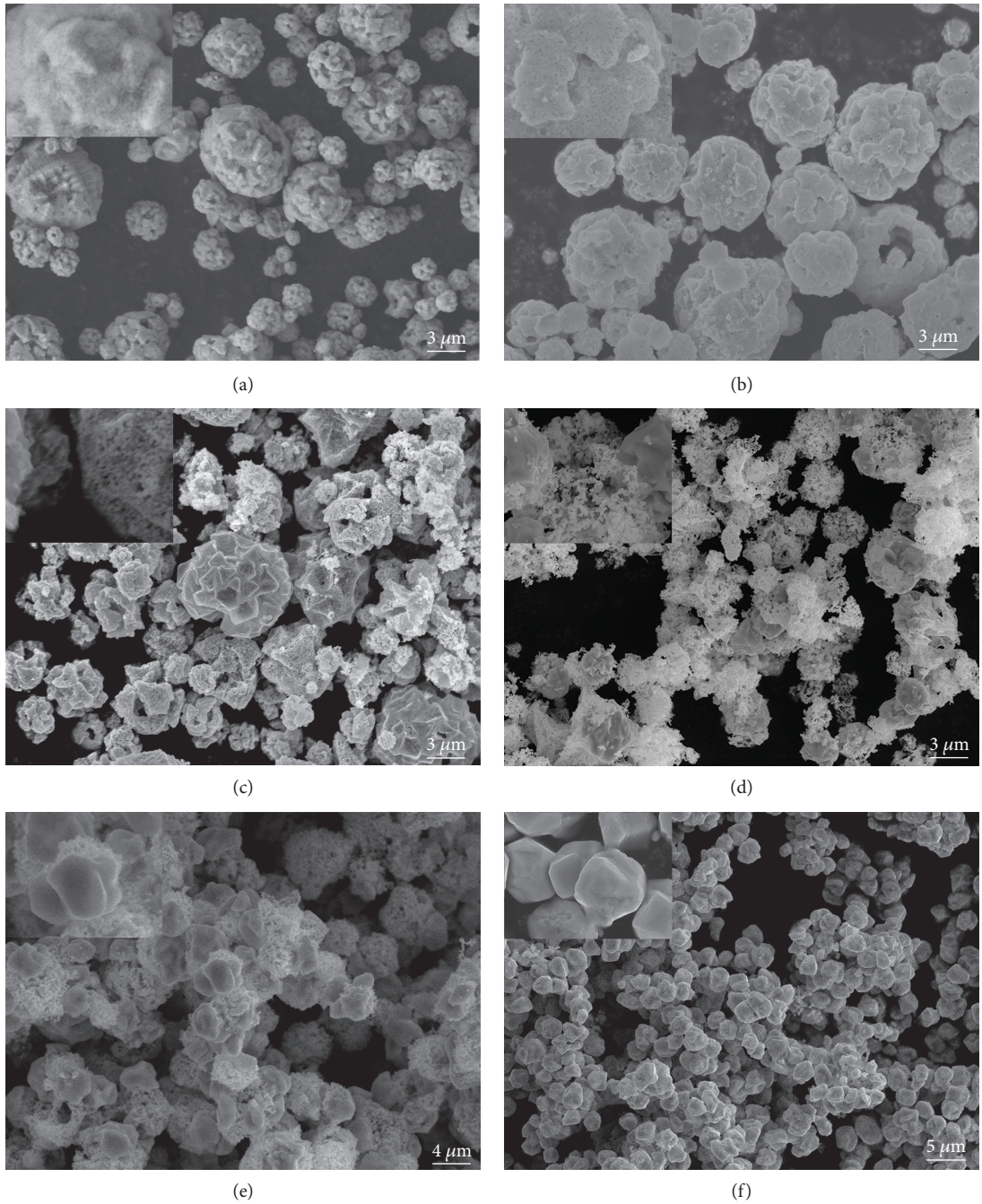

Figure 4: The microstructures of different thermal decomposition products of spray-dried $(NH_4)_2RuCl_6$ powder heated at (a) 300°C, (b) 345°C, (c) 385°C, (d) 410°C, (e) 450°C, and (f) 500°C.

near-spherical $(NH_4)_2PtCl_6$ particles can be achieved by spray-drying. The mean particle size of the spray-dried $(NH_4)_2PtCl_6$ powder is about 1.85 μm, and the particle size distribution ranges from 0.5 to 3.5 μm.

The microsized near-spherical $(NH_4)_2PtCl_6$ particles were totally transformed into Pt metal at 410°C, and the microstructure of thermal decomposition products was seriously influenced by different igniting temperatures. The results of this study show that the near-spherical high-purity ultrafine Pt particles with good dispersity and high density can be obtained by being ignited in N_2/H_2 (vol. 5 : 5) with a heating rate of 5°C/min at a temperature of 500°C for 30 min. The purity of the ignited ultrafine Pt particles was higher than 99.999 wt%, and the average size was about 1.12 μm. As-synthesized Pt particles meet the requirements of Pt paste fabrication. A further study will focus on the mechanism of the near-spherical ultrafine Pt particles formed from a Pt metal framework with mesoporous materials to the microsized lump Pt particles.

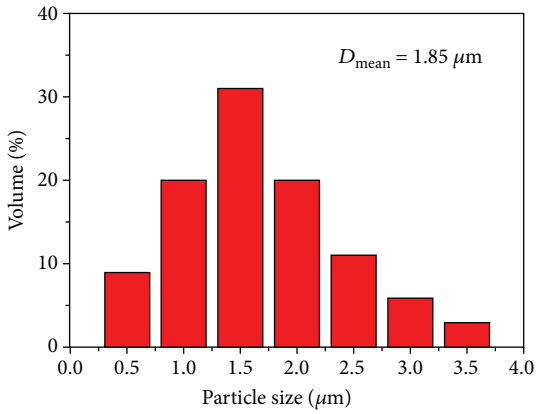

FIGURE 5: The particle size distribution of Pt powder at 500°C for 30 min.

Data Availability

Data is provided by the Northwest Institute for Non-ferrous Metal Research and Kunming Institute of Precious Metals.

Conflicts of Interest

All authors declare that we have no competing interests.

Authors' Contributions

This article was written by Panchao Zhao. Panchao Zhao, Wei Yi, and Qigao Cao gave ideas. The experiment was performed by Bosheng Zhang, Kunkun Chen, and Panchao Zhao.

Acknowledgments

This research was supported by funds from the National Natural Science Foundation of China (51864022), the Science and Technology Project of Yunnan Province-New Products (2016BA001), the State Key Laboratory of Advanced Technologies for Comprehensive Utilization of Platinum Metals (SKL-SPM-2018011), and Shaanxi Province Innovative Talent Promotion Program-Young Science and Technology Nova Project (2018KJXX-055). The authors thank the facilities and technical assistance of the Centre for Microscopy, Characterization, & Analysis at the Kunming Institute of Precious Metals.

References

[1] V. R. Stamenkovic, B. S. Mun, M. Arenz et al., "Trends in electrocatalysis on extended and nanoscale Pt-bimetallic alloy surfaces," *Nature Materials*, vol. 6, no. 3, pp. 241–247, 2007.

[2] N. Markovic, H. A. Gasteiger, and P. N. Ross, "Kinetics of oxygen reduction on Pt(hkl) electrodes: implications for the crystallite size effect with supported Pt electrocatalysts," *Journal of the Electrochemical Society*, vol. 144, no. 5, pp. 1591–1597, 1997.

[3] T. Toda, H. Igarashi, H. Uchida, and M. Watanabe, "Enhancement of the electroreduction of oxygen on Pt alloys with Fe, Ni, and Co," *Journal of the Electrochemical Society*, vol. 146, no. 10, pp. 3750–3756, 1999.

[4] K. Yahikozawa, Y. Fujii, Y. Matsuda, K. Nishimura, and Y. Takasu, "Electrocatalytic properties of ultrafine platinum particles for oxidation of methanol and formic acid in aqueous solutions," *Electrochimica Acta*, vol. 36, no. 5-6, pp. 973–978, 1991.

[5] M. Yuan, Z. Cui, J. Yang et al., "Ultrafine platinum nanoparticles modified on cotton derived carbon fibers as a highly efficient catalyst for hydrogen evolution from ammonia borane," *International Journal of Hydrogen Energy*, vol. 42, no. 49, pp. 29244–29253, 2017.

[6] M. Li, Z. Zhao, T. Cheng et al., "Ultrafine jagged platinum nanowires enable ultrahigh mass activity for the oxygen reduction reaction," *Science*, vol. 354, no. 6318, pp. 1414–1419, 2016.

[7] H. Wang, S. Lu, Y. Zhang, F. Lan, J. Shang, and Y. Xiang, "Platinum-decorated ultrafine Pd nanoparticles monodispersed on pristine graphene with enhanced electrocatalytic performance," *ChemPlusChem*, vol. 81, no. 2, pp. 172–175, 2016.

[8] X. He, Q. Chen, X. Xiong, X. Zhang, and Z. Nan, "Microstructure analysis of thick film platinum resistance paste during sintering," *Precious Metals*, vol. 28, pp. 28–31, 2007.

[9] N. H. Turner, "Investigation of the surface of platinum paste electrodes," *Journal of Electroanalytical Chemistry and Interfacial Electrochemistry*, vol. 87, no. 1, pp. 67–72, 1978.

[10] N. Okamoto, T. Hosoi, and K. Sakairi, "Method for recovering metal powder from platinum paste and method for regenerating platinum paste," 2017, EP 3121296.

[11] S. Achmatowicz, K. Kiełbasiński, E. Zwierkowska, I. Wyżkiewicz, V. Baltrušaitis, and M. Jakubowska, "A new photoimageable platinum conductor," *Microelectronics Reliability*, vol. 49, no. 6, pp. 579–584, 2009.

[12] C. Domínguez, K. M. Metz, M. K. Hoque et al., "Continuous flow synthesis of Pt nanoparticles in porous carbon as durable and methanol-tolerant electrocatalysts for oxygen reduction reaction," *ChemElectroChem*, vol. 5, no. 1, pp. 62–70, 2018.

[13] A. Carné-Sánchez, I. Imaz, M. Cano-Sarabia, and D. Maspoch, "A spray-drying strategy for synthesis of nanoscale metal-organic frameworks and their assembly into hollow superstructures," *Nature Chemistry*, vol. 5, no. 3, pp. 203–211, 2013.

[14] R. Vehring, "Pharmaceutical particle engineering via spray drying," *Pharmaceutical Research*, vol. 25, no. 5, pp. 999–1022, 2008.

[15] W. S. Cheow, S. Li, and K. Hadinoto, "Spray drying formulation of hollow spherical aggregates of silica nanoparticles by experimental design," *Chemical Engineering Research and Design*, vol. 88, no. 5-6, pp. 673–685, 2010.

[16] H. Xu, Z. Tan, H. Abe, and M. Naito, "Microcapsule assembly of single-walled carbon nanotubes from spray-dried hollow microspheres," *Journal of the Ceramic Society of Japan*, vol. 119, no. 1387, pp. 180–184, 2011.

[17] P. Luo and T. G. Nieh, "Synthesis of ultrafine hydroxyapatite particles by a spray dry method," *Materials Science and Engineering: C*, vol. 3, no. 2, pp. 75–78, 1995.

[18] J. Bi, W. Yi, J. Chen, M. Wen, and W. Guan, "Synthesis of high-purity micro-spherical ruthenium particles by chemical refining method," *Advanced Powder Technology*, vol. 27, no. 1, pp. 53–56, 2016.

[19] P. Zhao, J. Chen, Z. Xin, and W. Yi, "Synthesis and characterization of high-purity micro-spherical $(NH_4)_2RuCl_6$ particles using chemical separation combined with spray dried techniques," *Powder Technology*, vol. 317, pp. 275–280, 2017.

[20] R. D. Weir and E. F. Westrum Jr, "Thermodynamic properties of ammonium haloplatinates I. Heat capacity and thermodynamic functions of ammonium hexachloroplatinate $(NH_4)_2PtCl_6$ from 6K to 348K," *Journal of Chemical Thermodynamics*, vol. 22, no. 11, pp. 1097–1105, 1990.

[21] V. T. Yılmaz and H. Içbudak, "Thermal decomposition characteristics of ammonium hexachlorometallate(IV) complex salts of platinum metals," *Thermochimica Acta*, vol. 276, pp. 115–122, 1996.